Int. J. Appl. Math. and Comp. Sci., 2000, Vol.10, No.1, 157–173

CELLULAR AUTOMATA AND MANY-PARTICLE SYSTEMS MODELING AGGREGATION BEHAVIOR AMONG POPULATIONS†

DANIELA MORALE*

A cellular automaton model is presented in order to describe mutual interactions among the individuals of a population due to social decisions. The scheme is used for getting qualitative results, comparable to field experiments carried out on a population of ants which present an aggregative behavior. We also present a second description of a biological spatially structured population of N individuals by a system of stochastic differential equations of Itô type. A 'law of large numbers' to a continuum dynamics described by an integro-differential equation is given.

Keywords: cellular automata, individual-based models, stochastic differential equations, law of large numbers, density-dependence, nonlinear integro-differential equations

1. Introduction

In many animal species, individuals aggregate to form temporary or permanent groups, but how group cohesion is maintained and why groups assume a particular shape is not yet fully understood. Even if there exist some counterexamples, most observations of the dynamics of small and large groups show that coordination is locally controlled. It seems that more than long-range information transfer, global knowledge and external forces, the large scale patterns are due to the response of individuals to their local knowledge of environmental signals or markers or their neighbors (Gueron *et al.*, 1996; Partridge, 1982). As a consequence, it is an important problem to investigate the role of individual's social response to neighbors and to their local environment.

The motivation of our research comes from biological studies carried out by Boi (Boi and Capasso, 1997; Boi *et al.*, 2000) for a population of slave-maker ants of the species *Polyergus* rufescens. During their raids to the nests of other species of ants, the Amazons tend to aggregate in an organized army (transversal with respect to

† This word was partially supported by MURST (ex 40%) 'Processi stocastici e applicazioni' and CNR (Contract No. 97.00866.CT01) of Italy.

* Department of Mathematics, University of Milan, Via C. Saldini, 50, 20133 Milano, Italy, e-mail: morale@mat.unimi.it

the main direction of motion); they do not exhibit overcrowding effects. A relevant phenomenon is the spatial dependence of the social parameters on different environmental conditions, such as regularity of the terrain, reciprocal visibility, etc. which may impose restrictions on the sensory range among individuals.

It is often possible to consider continuum Eulerian models which describe only numbers of individuals per unit area or volume. For example, this is the case for large and dense aggregations of individuals. However, in many situations it is more appropriate to use discrete individual-based models in which a finite number of individuals is considered and only a finite sequence of decisions is made by individuals.

Anyway, as pointed out by Durrett and Levin (1994) or Grünbaum and Okubo (1994), an individual-based approach is useful in deriving the correct limiting equation, also in the case when the use of a continuum model can be justified. This is the aim of the present work. We build up some rules used by an individual in order to make decisions and we test them by means of a two-dimensional stochastic lattice-gas cellular automaton. First, by simple assumptions we consider the transition probability functions for each individual to go to the state $x + k\Delta x$ at time $t + \Delta t$, from the position x at time t, where $\Delta x, \Delta t$ are the mesh size and the time step. No external sources of information are assumed, as it would be present in the case of indirect physico-chemical signals (Stevens, 1992; 1996).

Here we deal with direct exchange of information between individuals about their positions within a bounded range of sensitivity. This means that each individual is supposed to perceive the spatial distribution of its neighbors in a finite neighborhood and may respond directly to their positions, densities or velocities (Grünbaum, 1994; Grünbaum and Okubo, 1994). At this stage we do not consider individuals having some inherent orientation (Deutsch, 1996).

Grünbaum (Grünbaum, 1994; Grünbaum and Okubo, 1994) presents a one-dimensional model for swarming; in this model it is assumed that individuals seek a target density, i.e. a desired number of neighbors in a predetermined neighborhood. Individuals count their neighbors and move in response to the gradient depending on how the observed density compares with the target density. Grünbaum's model is a variant of the 'additive type' models, in which the total force acting on each individual is the sum of many components including locomotory forces (constant swimming speed, viscous drag), aggregation or disaggregation forces (social attraction/repulsion between individuals), arrayal forces (tendency to match velocity or orientation of neighbors), deterministic environmental effects (directional tendencies, chemical gradients), random effects (behavioral and environmental stochasticity) (Okubo, 1986; Warburton and Lazarus, 1991).

Within the present work we introduce an additive force acting on each individual composed of aggregation and disaggregation forces and behavioral stochasticity; each particle is subject to random dispersal and compared to the Grünbaum-Okubo model, the peculiarity is that instead of a target density, we introduce a 'short-range' repulsion, while we keep the 'long-range' interaction for the aggregation term.

In Section 2, the biological phenomenon which we refer to is described. In Section 3, we introduce a cellular automaton model. Simulations exhibit the formation of

spatially stationary clusters, i.e. aggregation patterns whose number and radius size are strictly correlated with the size of the sensory distance considered. This qualitative behavior is compared with the field experimental results in (Boi and Capasso, 1997) (Section 4). In Section 5, we perform a heuristic derivation of a continuum model in which the neighborhood size for the aggregation term is a parameter that is not reducible to an infinitesimal limit contrary to the repulsion term. For the latter we get a *local* operator by reducing to zero the range of repulsion as the number of individuals is increasing. In Section 6, we refer to an interacting particle system used by the author to describe the same biological mechanism (Morale *et al.*, 1998a; 1998b). The process of animal grouping is continuous in time and space, but discrete in the population size. So the description of this phenomenon by a system of stochastic differential equations seems to be more natural. A rigorous derivation of a continuum model is given in (Morale *et al.*, 1998b).

2. A Biological Case

As an example of animal grouping we consider the aggregative behavior of the slave-maker ant *Polyergus* rufescens. The worker cast of this species is composed only of soldiers, unable to look after their nest. So they need to kidnap the pupae or newborn of few specific species. In order to keep constant the slave population in their nest, *Polyergus* ants periodically raid ant nests of the slave species. *Polyergus* soldiers aggregate in an army of 300–1000 individuals, 10–40 cm wide and some meters long. The army seems to be organized along the transversal component with respect to the main direction of the motion. In fact, in the main direction the dominant factor is the chemical trace produced by some scouts before the raid starts. On the return journey the ants walk single, with a variable distance between successive individuals. This means that there is a social response of each individual strictly related to the aim of the group. During the raids they need to be a big force so that they form a compact army. This is not necessary during their way back.

Analyzing the data obtained by fields observations (Boi and Capasso, 1997; Boi *et al.*, 2000), we can see remarkable differences in the army structure in different environmental conditions. In Fig. 1 the density profiles on four different types of ground based on morphological features are shown. From the top left to the bottom right, the density profiles on a plane area, black topped, an area covered only by small stones, an area covered by stones of all dimensional range and spot of grass, and an area covered by grass and all sort of tall and densely distributed obstacles are respectively shown. It is clear that the smaller the visibility range of each ant is (which corresponds to a poorer knowledge of the neighborhood), the stronger the force of aggregation. Our aim is to understand the rules of this behavior and how they depend on the sensory range of the ants.

3. A Cellular Automaton Model

We consider an aggregation model for biological populations. Aggregation is due to 'social' forces induced by the interaction of each individual with other individuals in

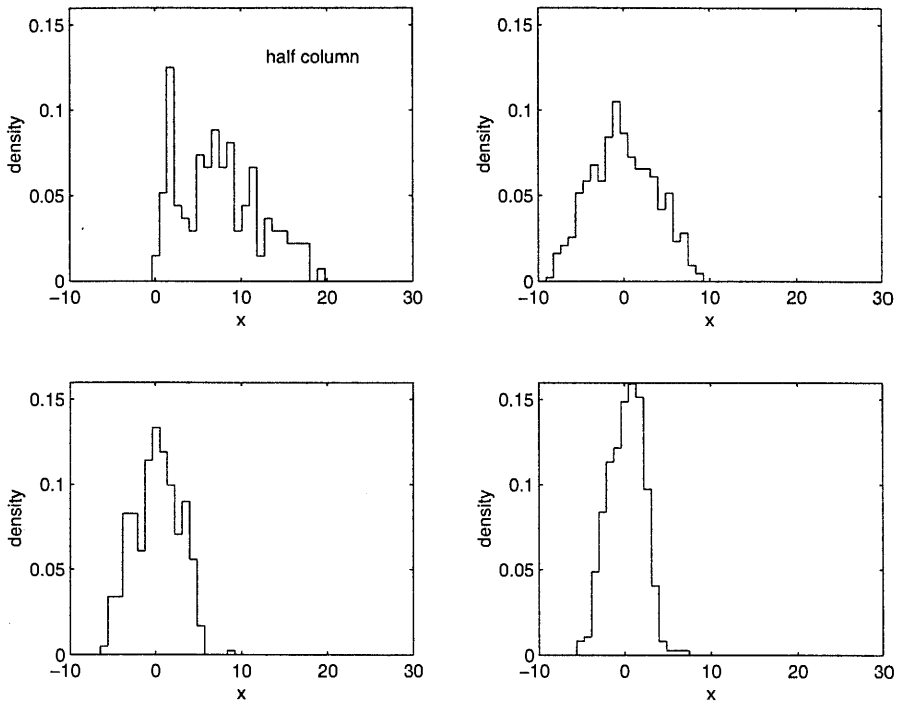

Fig. 1. 'Field'-experiments (Boi and Capasso, 1997): density profiles in a cross section of an army of *Polyergus* rufescens on different type of terrain: the number of obstacles is increasing, from a concrete ground in the top left-hand corner (where only half of the army is represented) to a high grass field in the bootom right-hand corner.

the population which belong to a suitable neighborhood. Instead of assuming a bounded target density of the population as in (Grünbaum, 1994), in our model we consider a short-range repulsion among individuals in order to prevent their accumulation in a single point in space.

In the cellular automaton model the particles are distributed randomly in an area of 100×100 units^2 with periodic boundary conditions. At each time step a particle performs the following actions:

1. Aggregation: it reacts to the density of other particles in a range of size R_a; the underlying assumption is that each particle is capable of perceiving the others only within this range;
2. Repulsion: it reacts to the density of other particles in a range of size R_r;
3. Diffusion: it moves randomly with coefficient σ_N which is decreasing when the number of particles increases.

The parameters R_a and R_r are chosen such that $R_r << R_a$, i.e. the region of repulsion is always strictly included in that of aggregation.

Define $A = \{1, \ldots, 100\}$. Let N be the total number of particles and let $N(x,t)$ count the number of particles in position x at time t. A detailed description of the evolution is presented further on. Furthermore, denote by $e_1 = (1,0)$, $e_2 = (0,1)$ the unit vectors spanning the plane.

3.1. Aggregation

Let $\Lambda_a(x) = \{y \in A^2 : |y - x| \leq R_a\}$ be the neighborhood of $x \in A^2$, in which all those particles contributing to the aggregation term of a particle in x are located. Moreover, for $i = 1, 2$, let

$$\Lambda_{a,+e_i}(x) = \{y \in \Lambda_a(x) : x_i < y_i\}$$

and

$$\Lambda_{a,-e_i}(x) = \{y \in \Lambda_a(x) : y_i < x_i\}.$$

This regions are shown in Fig. 2.

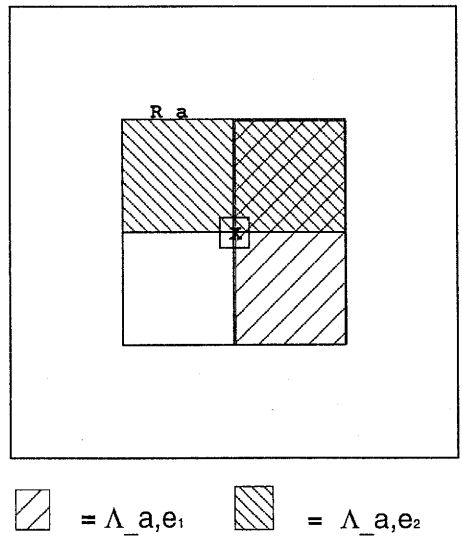

Fig. 2. The shaded regions are the neighborhoods $\Lambda_{a,+e_1}$ and $\Lambda_{a,+e_2}$.

Now, let $F_{a,r\,e_i}(x,t)$, $r = \pm$, $i = 1,2$ be the relative number of the particles in $\Lambda_{a,r\,e_i}(x)$, at time t, i.e.

$$F_{a,\pm e_i}(x,t) = \frac{1}{2N} \sum_{y \in \Lambda_{a,\pm e_i}(x)} N(y,t). \tag{1}$$

In (1) we introduce a normalization factor $1/N$. This also corresponds to associating the mass $1/N$ to each particle.

3.2. Repulsion

Let $\Lambda_r(x) = \{y \in A^2 : |y-x| \leq R_r\}$ be the neighborhood with radius R_r in which all those particles participating in the repulsion term of a particle in x are located. As we have motivated in Section 6, we consider a range of repulsion which is dependent on the total number of particles, in particular, we assume

$$R_r = N^{-\beta/2}, \qquad 0 < \beta < 1, \tag{2}$$

where β is a scaling parameter which determines the strength of interaction with the other particles. We refer to (Morale *et al.*, 1998a; 1998b) for a discussion on the consequences of different choices for β.

As before, let, for $i = 1, 2$,

$$\Lambda_{r,+e_i}(x) = \{y \in \Lambda_a(x) : x_i < y_i\}$$

and

$$\Lambda_{r,-e_i}(x) = \{y \in \Lambda_a(x) : y_i < x_i\}.$$

and let $F_{r,s\,e_i}(x,t)$, $s = \pm$, $i = 1, 2$ be the number of particles in the area $\Lambda_{r,s\,e_i}(x)$, at time t:

$$F_{r,\pm e_i}(x,t) = \frac{1}{2N} \sum_{y \in \Lambda_{r,\pm e_i}(x)} N(y,t). \tag{3}$$

3.3. Diffusion

We assume that the diffusion coefficient σ_N decreases as the number of particles increases. In particular, we suppose

$$\sigma_N = N^{-\alpha}, \quad \alpha \in (0,1). \tag{4}$$

By (4) we assume that if the number of particles is large enough, the mean free path of each particle does not have to be so large in order to make the particles enter into the area of interactions of the others. We also consider the relation between β and σ_N as given in a different form by (22):

i) $$0 < \beta < \frac{d}{d+2}$$

ii) $$\frac{d}{d+2} \leq \beta < 1, \qquad \alpha > \beta\frac{d+2}{d} - 1, \tag{5}$$

where d is the space dimension, i.e. $d = 2$. Denote by η and γ the strength of the response of the individuals to the 'social' forces, aggregation and repulsion, respectively. As discussed in (Boi and Capasso, 1997), they may depend on the range of aggregation. In particular, σ_N decreases like R_a^2 and γ like R_a. Throughout the section we consider the following rescaled coefficients:

$$\bar{\sigma}_N = \frac{\sigma_N}{R_a^2}, \quad \bar{\eta} = \frac{\eta}{R_a}, \quad \bar{\gamma} = \frac{\gamma}{R_a}.$$

which we denote respectively by σ_N, η and γ, for simplicity.

3.4. The Transition Probabilities

Each particle may move in four directions. Denote by δ and τ the mesh size and the time step, respectively. For numerical stability, we assume $\tau \leq \delta^2$. The probability for a particle in position x at time t to go to a position $x \pm e_i\delta$ at time $t + \tau$ is given by

$$P(x \pm e_i\delta; x, t) = \eta F_{a,\pm i}(x,t) + \frac{\gamma}{\Lambda_r} F_{r,\mp i}(x,t) + \frac{\sigma_N^2}{4}, \tag{6}$$

where

$$\Lambda_r = R_r^2. \tag{7}$$

In (6) we introduce, as stressed in the Introduction, *additive* weights for each possible direction; for the aggregation step the probability to go towards a larger density is higher, while for the repulsion step the probability to go towards lower concentrations is higher, as indicated by the index sign reversal. Furthermore, by the factor $1/\Lambda_r$ the strength of the repulsion becomes larger as $N \to \infty$. Finally, the random dispersal is added. The probability to stay in x is

$$P(x; x, t) = 1 - \sum_{i=1}^{2} P(x \pm e_i\delta; x, t). \tag{8}$$

4. Comparison with Experimental Data

As introduced, from the analysis of the social behavior of the ants of the species *Polyergus* rufescens, it is suggested that the spatial dependence of the social parameters depends on various environmental conditions, such as regularity of the terrain, reciprocal visibility, etc. Those environmental conditions may impose restrictions on the sensory range among individuals.

In Fig. 1, a significant difference of the profiles of the samples on different terrains is shown. The total width of the aggregation, measured by the transversal section, is 40 cm in the first terrain, without obstacles, where we see only half of the column of the army which does not show a strong concentration 20 cm on the terrain with few and small stones, about 12 cm on the third kind of terrain, where the number and the size of the stones are larger, and of about 11 cm in the terrain with high grass, i.e. with many and dense obstacles. So one can deduce that the more uneven the terrain is, the narrower the column of Amazons is. The absence of any plateau in the shown density profiles suggests that no target density exists, as assumed in the Grünbaum and Okubo model (Grünbaum, 1994; Grünbaum and Okubo, 1994).

In Fig. 3 we show the results of simulations of the cellular automaton model described above, by considering 1000 particles, the scaling parameter $\beta = 0.4$, and R_a equal to 75, 50, 20, 10 units, respectively. We can compare the patterns with the density profiles of the transversal sections of the army of ants in Fig. 1. As the sensory distance is increasing, fewer clusters are present, up to the complete disappearance of

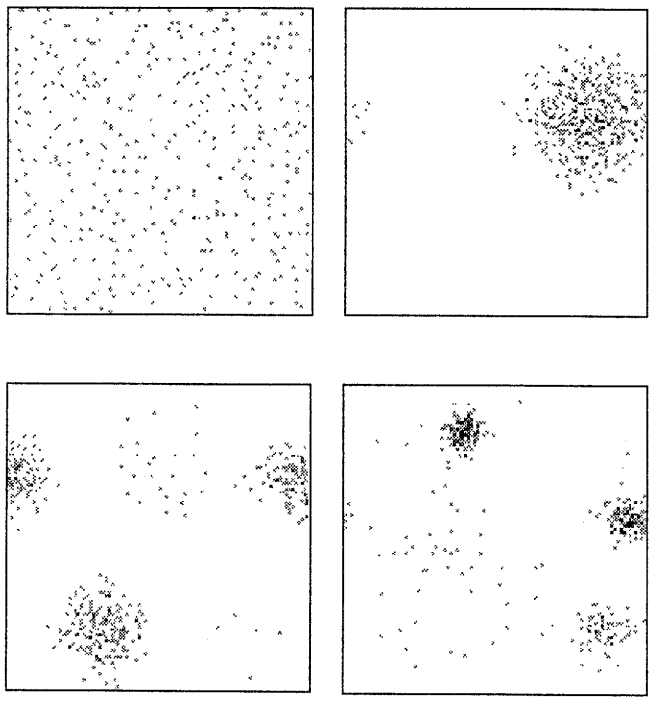

Fig. 3. Cellular automata simulations carried out on a 100 × 100 lattice, with a uniform initial condition, $N = 1000$. The range of aggregation R_a is, 75%, 50%, 20% and 10% of the edge of the lattice.

any phenomenon of aggregation. This last case can be compared to the first picture in Fig. 1, where the army does not show a strong concentration. As the number of clusters decreases, their radii become larger. This means that the aggregation force becomes weaker and weaker, as the sensory distance gets larger. The density at the boundary decreases slowly to zero in the first picture of Fig. 1, while it falls sharply on the other kind of terrains. That is exactly what happens in Fig. 3.

5. Heuristic Convergence of the Cellular Automaton Model to an Integro-Differential Equation

By considering the transition probabilities (6), (8) we observe that the expected number of particles in position x at time $t + \tau$ is given by

$$N(t+\tau, x) \sim N(t,x)P(x;x,t) + \sum_{k=1}^{2} N(t, x \pm e_k\delta)P(x; x \pm e_k\delta, t). \tag{9}$$

So, by Taylor expansions, we get

$$
\begin{aligned}
N(t+\tau,x) \;\sim\; & N(t,x) \\
& + \sigma_N^2\Big[- N(t,x) + \big(N(t,x+\delta e_1) + N(t,x-\delta e_1) \\
& + N(t,x+\delta e_2) + N(t,x-\delta e_2)\big)/4\Big] \\
& - \eta\Big[F_{a,e_1}(x,t) + F_{a,-e_1}(x,t) + F_{a,e_2}(x,t) + F_{a,-e_2}(x,t)\Big]N(t,x) \\
& - \frac{\gamma}{\Lambda_r}\Big[F_{a,e_1}(x,t) + F_{a,-e_1}(x,t) + F_{a,e_2}(x,t) + F_{a,-e_2}(x,t)\Big]N(t,x) \\
& + \eta\Big[F_{a,-e_1}(x+e_1\delta,t)N(t,x+e_1\delta) + F_{a,e_1}(x-e_1\delta,t)N(t,x-e_1\delta) \\
& + F_{a,-e_2}(x+e_2\delta,t)N(t,x+e_2\delta) + F_{a,e_2}(x-\delta e_2,t)N(t,x-e_2\delta)\Big] \\
& + \frac{\gamma}{\Lambda_r}\Big[F_{r,e_1}(x+e_1\delta,t)N(t,x+e_1\delta) - F_{r,-e_1}(x-e_1\delta,t)N(t,x-e_1\delta) \\
& + F_{r,e_2}(x+e_2\delta,t)N(t,x+e_2\delta) + F_{r,2}(x-e_2\delta,t)N(t,x-e_2\delta)\Big] \\
\simeq\; & N(t,x) + \sigma_N^2\delta^2\Delta N(t,x) \\
& - \sum_{k=1}^{2}\eta\Big[\big(F_{a,e_k}(x,t)N(t,x) - F_{a,e_k}(x-e_k\delta,t)N(t,x-e_k\delta)\big) \\
& - \big(F_{a,-e_k}(x+e_k\delta,t)N(t,x+e_k\delta) - F_{a,-e_k}(x,t)N(t,x)\big)\Big] \\
& + \frac{\gamma}{\Lambda_r}\sum_{k=1}^{2}\Big[\big(F_{a,e_k}(x+\delta e_k,t)N(t,x+\delta e_k) - F_{a,e_k}(x,t)N(t,x)\big) \\
& - \big(F_{a,-e_k}(x,t)N(t,x) - F_{a,-e_k}(x+\delta e_k,t)N(t,x-\delta e_k)\big)\Big]. \qquad (10)
\end{aligned}
$$

Consequently, we obtain

$$
\begin{aligned}
N(t+\tau,x) \;\sim\; & N(t,x) + \sigma_N^2\delta^2\Delta N(t,x) \\
& - \sum_{k=1}^{2}\eta\delta\Big[\nabla_{x_k}\big(F_{a,e_k}(x,t) - F_{a,-e_k}(x,t)\big)N(t,x)\Big] \\
& + \frac{\gamma\delta}{\Lambda_r}\sum_{k=1,2}\Big[\nabla_{x_k}\big(F_{r,e_k}(x,t) - F_{r,-e_k}(x,t)\big)N(t,x)\Big]. \qquad (11)
\end{aligned}
$$

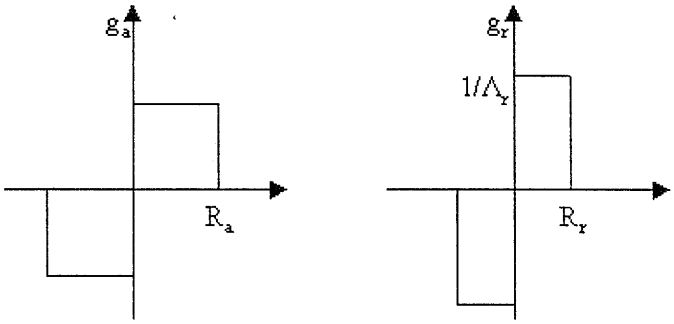

Fig. 4. Functions g_a and g_r in one dimension. They represent the kernels of aggregation and repulsion, respectively.

By considering the functions g_a and g_r as in Fig. 4, (11) becomes

$$\begin{aligned} N(t+\tau,x) \sim\ & N(t,x) + \sigma_N^2\delta^2\Delta N(t,x) \\ & + \frac{\eta\delta}{N}\Big[\nabla\big(N(t,\cdot) * g_a\big)(x)N(t,x)\Big] \\ & - \frac{\gamma\delta}{N}\Big[\nabla\big(N(t,\cdot) * g_r\big)(x)N(t,x)\Big], \end{aligned} \tag{12}$$

and so

$$\begin{aligned} \frac{N(t+\tau,x)-N(t,x)}{N\tau} \sim\ & \sigma_N^2\frac{\delta^2}{\tau}\Delta\frac{N(t,x)}{N} \\ & + \frac{\eta\delta}{\tau}\left[\nabla\Big(\frac{N(t,\cdot)}{N} * g_a\Big)(x)\frac{N(t,x)}{N}\right] \\ & - \frac{\gamma\delta}{\tau}\left[\nabla\Big(\frac{N(t,\cdot)}{N} * g_r\Big)(x)\frac{N(t,x)}{N}\right]. \end{aligned} \tag{13}$$

By (2) and (7), as $N \longrightarrow +\infty$, one gets

$$R_r \longrightarrow 0, \qquad \Lambda_r \longrightarrow +\infty, \qquad g_r \longrightarrow \nabla\delta,$$

where δ is the Dirac δ function.

If we consider $\eta, \beta \simeq \delta$ and $\delta^2 \simeq \tau$, by performing the limits $\delta, \tau \longrightarrow 0$ and $N \longrightarrow +\infty$ from (13), we obtain the following integro-differential equation:

$$\frac{\partial\rho}{\partial t}(x,t) = \sigma_\infty^2\Delta\rho(x,t) + \nabla\big((\rho(\cdot,t) * g_a)(x)\rho(x,t)\big) - \nabla\big(\rho(x,t)\nabla\rho(x,t)\big),$$

where $\lim_{N\to\infty}\sigma_N = \sigma_\infty$ and $\rho(t,x)$ is the probability density for $N(t,x)$. Assuming $\sigma_\infty = 0$ as $N \longrightarrow +\infty$, we get

$$\frac{\partial\rho}{\partial t}(x,t) = \nabla\big((\rho(\cdot,t) * g_a)(x)\rho(x,t)\big) - \nabla\big(\rho(x,t)\nabla\rho(x,t)\big). \tag{14}$$

6. An Individual-Based Model

In this section we refer briefly to (Morale *et al.*, 1998a; 1998b). We start from the Lagrangian description of a system of $N(\in \mathbb{N} \setminus \{0\})$ particles by their random locations at time t. Suppose the k-th particle ($k \in \{1, \ldots, N\}$) is located at $X_N^k(t)$ at time $t \geq 0$; each $X_N^k(t)$ is an $\mathbb{R}^d$-valued random variable defined on a common probability space $(\Omega, \mathcal{F}, P)$.

The distribution of the system of N particles at time t is described by the random measure on $\mathbb{R}^d$

$$X_N(t) = \frac{1}{N} \sum_{k=1}^{N} \epsilon_{X_N^k(t)}, \tag{15}$$

which is known as the *empirical measure* of the system of N particles at time t; it attributes the mass $1/N$ to each particle of the system.

Correspondingly, the measure-valued process

$$X_N : t \in \mathbb{R}_+ \longrightarrow X_N(t) = \frac{1}{N} \sum_{k=1}^{N} \epsilon_{X_N^k(t)}$$

is known as the *empirical process* of the system. The Lagrangian description of the dynamics of our system of interacting particles is given via a system of stochastic differential equations as follows:

$$\mathrm{d}X_N^k(t) = F\big[X_N(t)\big]\big(X_N^k(t)\big)\mathrm{d}t + \sigma_N \mathrm{d}W^k(t), \quad k = 1, \ldots, N, \tag{16}$$

where we assume that the k-th particle is subject to random dispersal described by the Brownian motion W^k.

We assume that $\{W^k(\cdot),\ k = 1, 2, \ldots\}$ is a family of independent standard Wiener processes. Furthermore, we assume that the common variance σ_N^2 depends on the total number of particles.

The drift term F describes the specific dynamics of the system of interacting particles, based on our modeling assumptions. In particular, we assume that it depends on the location of the respective particle and on the empirical measure $X_N(t)$ of the system of all particles at time t. We may express Assumptions 1–3 in Section 1 by introducing in the drift term F two components: F_1, responsible for aggregation, and F_2, describing the repulsion, such that

$$F = F_1 + F_2.$$

6.1. The Aggregation Term F_1

First, we introduce a convolution kernel

$$G_a : \mathbb{R}^d \longrightarrow \mathbb{R}_+,$$

concentrated essentially in the ball centered at $0 \in \mathbb{R}^d$ with radius R_a, which corresponds to the range of sensitivity for aggregation. G_a is supposed to be independent of N.

We assume that the aggregation term F_1 depends on a 'generalized gradient' of $X_N(t)$ at $X_N^k(t)$:

$$F_1\big[X_N(t)\big]\big(X_N^k(t)\big) = \big[\nabla G_a * X_N(t)\big]\big(X_N^k(t)\big). \tag{17}$$

This means that each individual feels the nonlocal (smoothed) gradient of the measure $X_N(t)$ around itself via the kernel G_a; the positive sign for F_1 means that it models a force of attraction of the particles in the direction of an increasing concentration of neighbors.

6.2. The Repulsion Term F_2

As far as repulsion is concerned, we proceed in a similar way by introducing a convolution kernel

$$V_N : \mathbb{R}^d \longrightarrow \mathbb{R}_+,$$

which determines the range and the strength of the influence of neighboring particles.

We assume (by anticipating a possible limiting procedure) that V_N depends on the total number N of interacting particles as follows:

$$V_N(x) = \chi_N^d V_1(\chi_N x), \quad x \in \mathbb{R}^d,$$

where V_1 is a probability density on $\mathbb{R}^d$, and χ_N is a scaling parameter that we choose as

$$\chi_N = N^{\beta/d}, \tag{18}$$

where $\beta \in (0,1)$. It is clear that

$$\lim_{N\to+\infty} V_N = \delta_0, \tag{19}$$

where δ_0 is Dirac's delta function.

Finally, we assume that

$$\begin{aligned} F_2\big[X_N(t)\big]\big(X_N^k(t)\big) &= -\big(\nabla V_N * X_N(t)\big)\big(X_N^k(t)\big) \\ &= -\frac{1}{N}\sum_{m=1}^{N} \nabla V_N\big(X_N^k(t) - X_N^m(t)\big). \end{aligned} \tag{20}$$

This means that each individual feels a nonlocal (smoothed) gradient of the population in a small neighborhood. F_2 provides a drift toward a decreasing concentration of the population; its range is decreasing as the size of the population increases.

In Figs. 5–8 we present some simulations of the system of stochastic differential equations (16), (17) and (20).

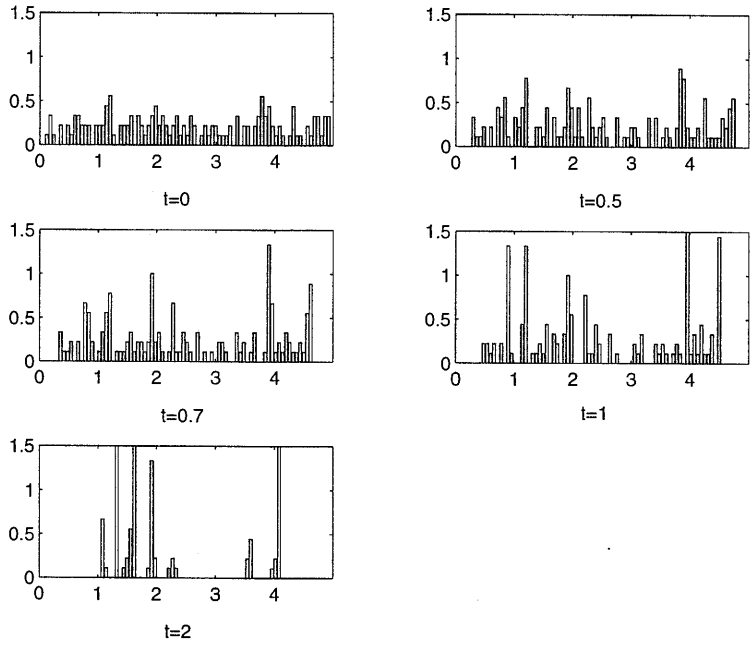

Fig. 5. Time evolution results for the SDE model with a uniform initial distribution: $R_a = 1$.

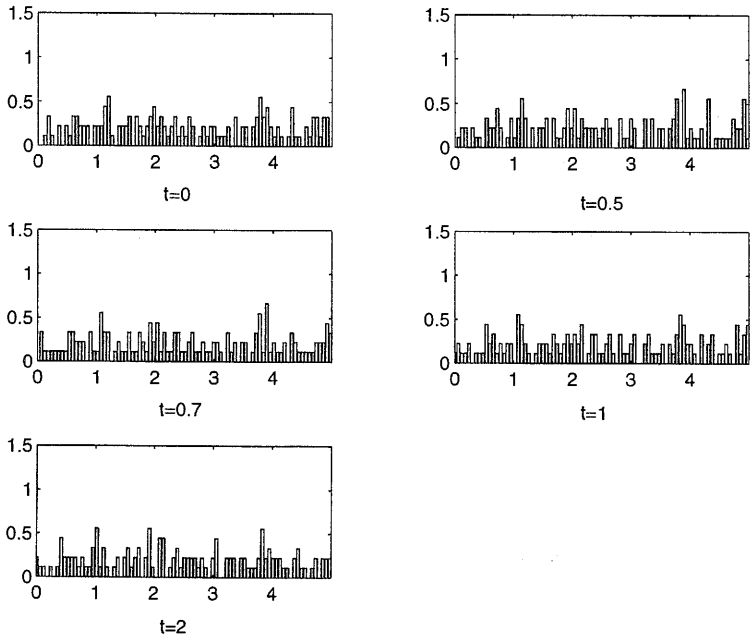

Fig. 6. Time evolution results for the SDE model with a uniform initial distribution: $R_a = 4$.

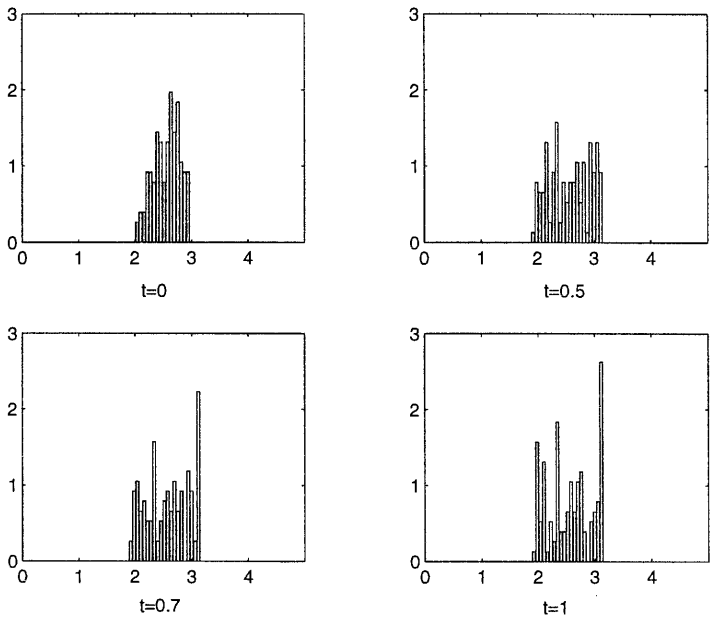

Fig. 7. Time evolution of the population density for the SDE model with a beta initial distribution: $R_a = 2$.

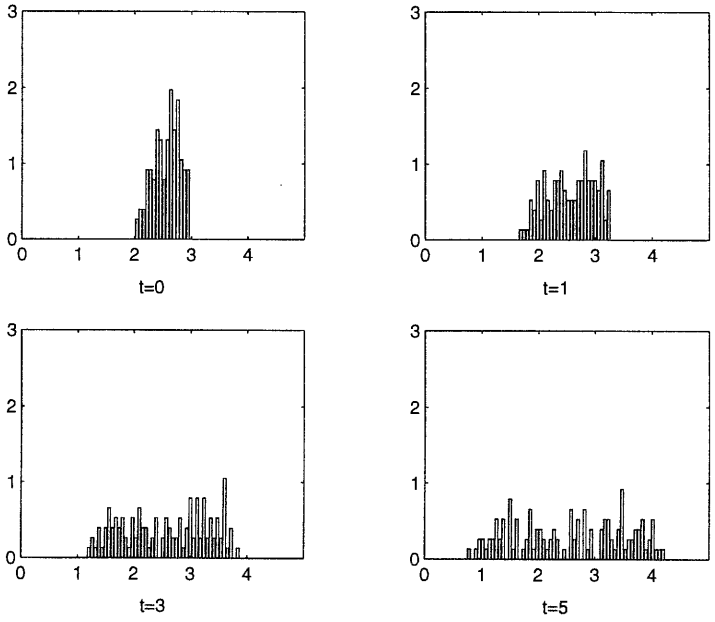

Fig. 8. Time evolution of the population density for the SDE model with a beta initial distribution: $R_a = 4$.

Figures 5 and 6 show the time evolution of a unit mass initially uniformly distributed in the interval $[0,5]$. Sensory ranges $R_a = 1$ and $R_a = 4$ are considered respectively. Figure 5 shows a formation of clusters, while in Fig. 6 the density is still uniformly distributed. This confirms again our conjecture: the aggregation phenomenon in the case studied is stronger when the sensory distance of particles is smaller.

In Figs. 7 and 8, a beta initial distribution is considered, with $R_a = 2$ and $R_a = 4$ respectively. This means that initially all particles are located within an interval of radius equal to 1. So, in order to avoid overcrowding effects, they repel. Hence the shapes of the profiles become smoother and the high peak tends to vanish. In any case, in Fig. 7 the group goes on being compact because of the stronger aggregation forces.

In (Morale *et al.*, 1998a) we prove a law of large numbers to a continuum model. Let us consider the following assumption:

Assumption 1. *For some $T \in [0,\infty)$ system (24) admits a unique, nonnegative solution $\rho \in C_b^{[(d+2)/2]+2,1}(\mathbb{R}^d \times [0,T])$. Together with its partial derivatives of order $\leq [(d+2)/2]+1$, the solution ρ is integrable uniformly on $t \leq T$.*

Let us consider the following assumptions for the kernel of aggregation G_a:

$$G_a \in C_b^{[(d+2)/2]+2}(\mathbb{R}^d). \tag{21}$$

As far as β is concerned, we need to assume either of the following two conditions:

$$\begin{aligned} &\text{i)} \quad \beta < \frac{d}{d+2}, \quad \inf_N \sigma_N > 0, \quad \lim_{N\to\infty} \sigma_N = \sigma_\infty < \infty, \\ &\text{ii)} \quad \beta > \frac{d}{d+2}, \quad \lim_{N\to+\infty} \sigma_N N^{\beta(d+2)/d-1} = 0. \end{aligned} \tag{22}$$

Let $h_N(x,t) = X_N(t) * V_N$ be a regularized version of the measure $X_N(t)$.

Theorem 1. (Morale *et al.*, 1998a) *Under Assumption 1, and assumptions (21) and (22), if*

$$\lim_{N\to\infty} E\Big[\|h_N(\cdot,0) - \rho_0(\cdot)\|_2^2\Big] = 0,$$

then

$$\lim_{N\to\infty} E\Big[\sup_{t\leq T} \|h_N(\cdot,t) - \rho(\cdot,t)\|_2^2\Big] = 0, \tag{23}$$

where ρ is the unique solution of

$$\begin{aligned} \frac{\partial}{\partial t}\rho(x,t) &= \frac{\sigma_\infty^2}{2}\Delta\rho(x,t) + \nabla\cdot\big(\rho(x,t)\nabla\rho(x,t)\big) \\ &\quad - \nabla\cdot\Big[\rho(x,t)\big(\nabla G_a * \rho(\cdot,t)\big)(x)\Big], \quad x\in\mathbb{R}^d, \ t\geq 0, \\ \rho(x,0) &= \rho_0(x), \quad x\in\mathbb{R}^d. \end{aligned} \tag{24}$$

Equation (23) implies

$$\lim_{N\to\infty} \langle X_N(t), f\rangle = \langle X(t), f\rangle = \int f(x)\rho(x,t)\,\mathrm{d}x \tag{25}$$

uniformly in $t \in [0,T]$, *for any* $f \in C_b^1(\mathbb{R}^d) \cap L^2(\mathbb{R}^d)$.

The proof (Morale *et al.*, 1998a) is based on the direct estimation of the term $\|h_N(x,t) - \rho(x,t)\|_2^2$ by means of Itô's formula and Doob's inequality. After the L^2 convergence of the regularized measure h_N is obtained, it becomes easy to prove the weak convergence of X_N. The interested reader can refer to (Morale *et al.*, 1998a; 1998b) for more details.

Acknowledgments

It is a great pleasure to acknowledge fruitful discussions with Prof. Vincenzo Capasso, Dr. Karl Oelschläger, Andreas Deutsch and the work group of Prof. W. Jäger during my wonderful staying at University of Heidelberg. Thanks are also due to Silvia Boi for relevant discussions on the biological mechanisms involved in my research.

References

Boi S. and Capasso V. (1997): *The aggregative behavior of the species Polyergus rufescens latr.: From the observations to the mathematical model.* — Quaderno No.37/1997, Dipartimento di Matematica, Universitá di Milano (in Italian).

Boi S., Capasso V. and Morale D. (2000): *Modeling the aggregative behavior of ants of the species Polyergus rufescens.* — J. Nonlin. Anal., Series B (to appear).

Deutsch A. (1996): *Orientation-induced pattern formation: Swarm dynamics in a lattice gas automaton model.* — Int. J. Bifurc. Chaos, Vol.6, No.9, pp.1735–1752.

Durrett R. and Levin S.A. (1994): *The importance of being discrete (and spatial).* — Th. Pop. Biol., Vol.46, pp.363–394.

Grünbaum D. (1994): *Translating stochastic density-dependent individual behaviour with sensory constraints to an Eulerian model of animal swarming.* — J. Math. Biol., Vol.33, pp.139–161.

Grünbaum D. and Okubo A. (1994): *Modelling social animal aggregations*, In: Frontiers of Theoretical Biology (S. Levin, Ed.). — Lectures Notes in Biomath., Vol.100, New York: Springer Verlag, pp.296–325.

Gueron S., Levin S.A. and Rubenstein D.I. (1996): *The dynamics of herds: From individuals to aggregations.* — J. Theor. Biol., Vol.182, pp.85–98.

Morale D., Capasso V. and Oelschläger K. (1998a): *A rigorous derivation of a nonlinear integro-differential equation from a SDE for an aggregation model.* — Preprint 98–38 (SFB 359), IWR, University of Heidelberg.

Morale D., Capasso V. and Oelschläger K. (1998b): *On the derivation of the mean-field nonlinear integro-differential equation for a population of aggregating individuals subject to stochastic fluctuations.* — Preprint 98–39 (SFB 359), IWR, University of Heidelberg.

Okubo A. (1986): *Dynamical aspects of animal grouping: swarms, school, flocks and herds.* — Adv. BioPhys., Vol.22, pp.1–94.

Partridge B.C. (1982): *The structure and function of fish schools.* — Sci. Amer., Vol.246, pp.114–123.

Stevens A. (1992): *Mathematical modelling and simulations of the aggregation of Myxobacteria. Chemotaxis-equations as limit dynamics of moderately interacting stochastic processes.* — Ph.D. Th., Institut für Angewandte Mathematik, Universität Heidelberg.

Stevens A. (1996): *Simulations of chemotaxis-equations in two space dimensions*, In: Nonlinear Physics of Complex Systems — Current Status and Future Trends (J. Parisi, S.C. Mueller, and W. Zimmermann, Eds.). — Berlin: Springer Verlag.

Warburton K. and Lazarus J. (1991): *Tendency-distance models of social cohesion in animal groups.* — J. Theor. Biol., Vol.150, pp.473–488.